

Interannual changes of active fire detectability in North America from long-term records of the advanced very high resolution radiometer

Ivan Csiszar,^{1,2} Abdelgadir Abuelgasim,^{3,4} Zhanqing Li,⁵ Ji-zhong Jin,⁵ Robert Fraser,⁶ and Wei-Min Hao⁷

Received 10 October 2001; revised 20 February 2002; accepted 21 February 2002; published 31 January 2003.

[1] This paper addresses practical issues related to the processing of 1-km National Oceanic and Atmospheric Administration (NOAA) advanced very high resolution radiometer (AVHRR) data for producing a consistent, long-term time series of active fire locations over the Continental United States and Canada. The effects of the interannual changes in measured background temperatures, caused by the orbital drift of the afternoon NOAA satellites and by environmental factors, are investigated. Background temperature changes are analyzed using a time series of monthly mean clear-sky brightness temperatures from the NOAA National Environmental Satellite, Data, and Information Service (NESDIS) Pathfinder Atmosphere (PATMOS) data set at a $1^\circ \times 1^\circ$ resolution. Examples of target areas over four predominant land cover types, as defined in the International Geosphere-Biosphere Programme (IGBP) global 1 km data set, are presented. The results indicate that over forests (defined as >60% tree canopy cover) the contrast between nonburning background and fire pixels is nearly always sufficient for successful fire detection. Over nonforested areas, however, the low saturation temperature of the mid-IR channel on the NOAA 7 to NOAA 14 satellites often sets a physical limit to the separation of valid fire pixels and false ones. Moreover, the severity of this effect changes over the years with the changing background temperatures. The results suggest that because of the potential spurious trends in the number of fires, nonforested areas be excluded from the multiyear analysis. However, a detailed assessment of the emissions from nonforest fires is needed to quantify the effect of this on continental-scale emission estimates. *INDEX TERMS:* 0315 Atmospheric Composition and Structure: Biosphere/atmosphere interactions; 1615 Global Change: Biogeochemical processes (4805); 1640 Global Change: Remote sensing; 1694 Global Change: Instruments and techniques; *KEYWORDS:* AVHRR, biomass burning, satellite fire detection, interannual variability

Citation: Csiszar, I., A. Abuelgasim, Z. Li, J. Jin, R. Fraser, and W.-M. Hao, Interannual changes of active fire detectability in North America from long-term records of the advanced very high resolution radiometer, *J. Geophys. Res.*, 108(D2), 4075, doi:10.1029/2001JD001373, 2003.

1. Introduction

[2] Active fire detection and burned area mapping have become major issues in terrestrial carbon research. Biomass burning in the tropics is a significant source of organic

carbon to the atmosphere [Hao *et al.*, 1996; Fearnside, 2000]. However, emissions from boreal forest fires in North America and Siberia and agricultural and nonforested wild-fires are believed to be more important than previously thought [Cofer *et al.*, 1996; Lobert *et al.*, 1999; Dwyer *et al.*, 2000]. To estimate emissions from fires, information on the amount of fuel and the corresponding combustion efficiency is needed. The amount of fuel consumed can be estimated from the burned area and from the type and density of fuel (i.e., vegetation) within the burned area. Vegetation cover has been generally characterized over most of the Earth's surface both from ground surveys and satellite observations [Cihlar, 2000]. Similarly, there have been advances in determining burning efficiencies and emission factors for various fuel types [Andreae and Merlet, 2001].

[3] Large-scale observation of fires is feasible in most cases only by means of satellite measurements. A long-term satellite-based fire inventory on a continental to global scale, however, is currently not available. The longest such

¹Cooperative Institute for Research in the Atmosphere, Office of Research and Applications, National Environmental Satellite, Data, and Information Service, National Oceanic and Atmospheric Administration, Camp Springs, Maryland, USA.

²Now at Department of Geography, University of Maryland, College Park, Maryland, USA.

³Intermap Technologies, Ottawa, Ontario, Canada.

⁴Now at Noetix Research Inc., Ottawa, Ontario, Canada.

⁵Department of Meteorology, Earth System Science Interdisciplinary Center, University of Maryland, College Park, Maryland, USA.

⁶Canada Center for Remote Sensing, Ottawa, Ontario, Canada.

⁷Fire Sciences Laboratory, USDA Forest Service, Missoula, Montana, USA.

data record currently is the nighttime-only World Fire Atlas from measurements of the Along Track Scanning Radiometer (ATSR), which goes back to 1995 [Arino *et al.*, 2001]. However, there is the potential to extend the retrospective inventory over a 10–15 year period using the continuous data records from operational environmental satellites. Of particular significance are the midinfrared data from the polar orbiter NOAA (National Oceanic and Atmospheric Administration; Kidwell [1998]) and geostationary GOES [Prins *et al.*, 1998], and nighttime visible observations from DMSP (Defense Meteorological Satellite Program) [Elvidge *et al.*, 2001]. The relative merits of these data sets have been discussed by Gutman *et al.* [2001].

[4] Overall, the advanced very high resolution radiometer (AVHRR/2; or AVHRR for brevity) onboard the NOAA satellites is the most suitable instrument for long-term, large-scale fire mapping. To date, two global-scale fire inventories have been derived from AVHRR: the Global Fire Product [Stroppiana *et al.*, 2000] covering the years 1992 and 1993, and the World Fire Web system, which started in 1998 [Grégoire *et al.*, 2001]. Active fire products are included in the AVHRR Land Pathfinder II processing system [El Saleous *et al.*, 2000], yet a long-term record from this product is not available. In addition, several countries operate national AVHRR-based fire monitoring systems, including those in Canada [Li *et al.*, 2000a] and in Brazil [Franca and Setzer, 2001].

[5] AVHRR provides measurements in 5 channels in the visible (R1; 0.58 μm), near-infrared (R2; 0.9 μm), midinfrared (T3; 3.7 μm) and thermal infrared (T4; 10.5 μm and T5; 11.5 μm) spectral regions (in this paper “R” and “T” denote top-of-the-atmosphere reflectances and brightness temperatures respectively). The data are available at two resolutions. The original nominal resolution of AVHRR is 1 km, and in most situations fire detection is effective only at this resolution. Real-time 1-km data are continuously transmitted as part of the High-Resolution Picture Transmission (HRPT) data stream, which can be acquired by local direct-readout receiving stations. 1-km data from select areas and time periods are also recorded on board the satellite and then transmitted as Local Area Coverage (LAC) data. The Global Area Coverage (GAC) data are created on board the satellite by the spatial sampling and averaging of the original resolution measurements into a nominal 4 km resolution [Kidwell, 1998]. Except from large fires [Belward *et al.*, 1994], GAC data are not useful for a quantitative assessment of fires; however, they can be used for regional to global scale studies of surface changes [Barbosa *et al.*, 1999]. GAC data represent a nearly complete temporal and global spatial coverage since the early 1980s. Although long time series of 1-km AVHRR data are not available globally, continental-scale databases can be processed into a meaningful inventory, particularly over North America, where a nearly continuous data record starting in 1985 has been compiled and maintained by NOAA [Gutman *et al.*, 2001].

[6] There have been numerous studies on the detection of active fires from AVHRR, utilizing the sensitivity of its midinfrared (3.7 μm) channel radiance to hot objects that may cover only a small fraction of a pixel [Dozier, 1981; Robinson, 1991]. While AVHRR measurements are available both at daytime and at nighttime, daytime observations

have been preferred because they were coincident with the peak of the diurnal fire activity in many regions, particularly in the tropics. This, however, introduces two major limitations. First, the daytime radiance signal at 3.7 μm is a combination of useful emitted thermal radiation and a reflected solar component, the latter of which may elevate the signal to a high enough level to produce false fire alarm. Second, the radiation from hot background surface and/or increased solar reflection can saturate the 3.7 μm channel of AVHRR [Grégoire *et al.*, 1993]. According to technical documentation, the prelaunch 3.7 μm channel saturation temperature is ~ 320.5 K, 322.0 K, 321.5 K and 321.5 K respectively [Csiszar and Sullivan, 2002] for the “afternoon” NOAA satellites: NOAA 7, 9, 11 and 14. (Over the satellite’s lifetime, the actual saturation temperature shows some increase with sensor degradation.) Because of this small intersatellite variability, in this paper we use a constant saturation temperature of 322 K. Paradoxically, the saturation temperatures of channels 4 and 5, which are far less likely to reach this brightness temperature value, have a ~ 5 – 8 degrees higher nominal saturation temperature. These channels can be significantly elevated only by very large subpixel fires [Li *et al.*, 2001].

[7] Note that earlier studies have reported a problem in the onboard signal processing on some NOAA satellites for bright and hot objects that saturated the 3.7 μm sensor, resulting spuriously lower brightness temperatures than the nominal saturation value [Setzer and Verstraete, 1994; Harris *et al.*, 1995]. This phenomenon introduces a further limitation in AVHRR-based fire detection, but does not effect the conclusions of this paper. Thus it is not discussed in further detail here.

[8] Most of the techniques for fire detection separate the real fire signal from the false alarm using spectral and spatial information [Li *et al.*, 2001]. Although some of these were designed for global applications, tuning of the thresholds to local conditions is necessary to reach a reasonable compromise between omission and commission errors. In general, the detection accuracy over forested areas is higher than in nonforested areas, where surface heating and reflection can be substantial.

[9] The mapping of burned areas from satellite is based on the detection of surface reflectance changes within a certain period of time [Zhan *et al.*, 2000]. The most commonly used parameter derived from AVHRR measurements to characterize land surface conditions is the Normalized Difference Vegetation Index (NDVI) [Fernandez *et al.*, 1997]; although other very promising techniques also exist [Roy and Lewis, 2000]. For large fires over dense vegetation, the burned area signal from the temporal change of NDVI remains for a longer time period and is less subject to the omission errors of active fire detection (obscuration by clouds or heavy smoke, insufficient temporal coverage etc.). Thus it provides a more accurate estimate of burned areas than a cumulative area from detected active fires. However, coincident mapping of active fires is still useful. For example, the Hotspot and NDVI Differencing Synergy (HANDS) algorithm, developed for Canadian boreal forests by Fraser *et al.* [2000] requires the presence of detected active fire pixels within potential burned area polygons with substantial NDVI decrease to avoid false signal from surface changes that

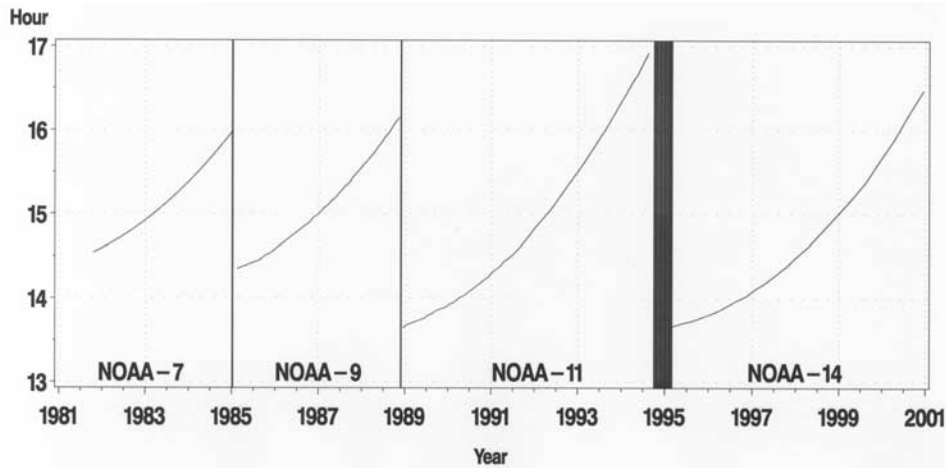


Figure 1. Equator crossing times of the “afternoon” NOAA satellites over the 1981–2000 period.

are not fire related, such as droughts. Active fire detection is also useful to map small, subpixel agricultural fires where the NDVI differencing is not suitable for burned area mapping. *Barbosa et al.* [1999] used the active fire data from the Global Fire Product [*Stroppiana et al.*, 2000] for large-scale validation of their multithreshold, multitemporal Burned Area Algorithm over Africa.

[10] The primary objective of this study is to discuss the different issues related to the potential for deriving a reliable long-term inventory of active fires that can be used for burned area confirmation or validation purposes. To achieve a high-quality time series of active fire occurrences, we need to ensure not only that detection errors are minimized but also that they are consistent over the years. The omission and commission errors are strongly related to the separability of the fire signal from the background conditions; thus interannual change of background conditions may introduce biases in detection accuracy.

[11] There are two major factors that contribute to the interannual change of background conditions: (1) the orbital drift of the NOAA satellites (i.e., the gradual change of the equator crossing time over the years; Figure 1), which results in varying local time of observation and in varying illumination angles and (2) natural interannual change in meteorological conditions. This study mainly focuses on the first effect; however, the empirical data analysis presented below also integrates the second effect. Note that the recording of fire observations at different local times also results in different sampling of the diurnal cycle of fires, particularly of those of relatively short duration over non-forested areas. This effect will not be discussed in this paper.

[12] The interannual change in the local time of observation yields varying background temperatures and thus a varying degree of temperature contrast between fire pixels and their background. The change in illumination angle contributes to the change of reflected component in the midinfrared radiance, which normally is similar in magnitude to the thermally emitted radiance component, and also to the occurrence of sun-glint conditions (i.e., specular reflection from water surfaces). This latter effect is particularly important in the presence of subpixel scale water

bodies, a typical condition, for example, in the Canadian boreal forest region, where a decision needs to be made whether to exclude such pixels from the analysis at the expense of potentially excluding real fires.

[13] In this paper we present analysis of the interannual changes of background conditions. Effects of the interannual changes in sun-glint occurrence are considered of secondary importance and are not discussed. Our focus is North America, particularly the diverse ecosystems of the conterminous United States. Section 2 provides a description of the AVHRR Pathfinder Atmosphere (PATMOS) data set, which was used to characterize background temperature conditions. In section 3 an analysis of the time series of daytime clear-sky background brightness temperatures is presented. Section 4 presents a case of extensive burning over nonforested areas. Concluding remarks can be found in section 5.

2. AVHRR Pathfinder Atmosphere (PATMOS) Data Set

[14] In this analysis we used data from the NOAA/NESDIS Pathfinder Atmosphere (PATMOS) data set [*Stowe et al.*, 2002]. This data set is now available from mid-1981 to the end of 2000, covering the “afternoon” satellites of the NOAA polar orbiter series. A number of products were derived daily from AVHRR GAC data, aggregated into daytime and nighttime mean values on a global 10,000 km² equal-area grid and averaged over five-day and monthly time periods. Although the primary objective of this data set has been the derivation of cloud and aerosol products, its clear-sky radiance products can be used for the analysis of land surface processes, as demonstrated by *Gutman et al.* [2000]. Note that we use PATMOS data to characterize spatially relatively homogeneous background temperature conditions and thus the use of a GAC-based data set is appropriate. In the current analysis we used daytime, monthly mean, clear-sky, top-of-the-atmosphere AVHRR channel 3 and channel 4 radiance products, reprojected onto a 1° × 1° global grid. The radiance values were converted into brightness temperatures using satellite-specific centroid wavenumbers and conversion coefficients.

We made the a priori assumption that the number of fire pixels within a given $1^\circ \times 1^\circ$ cell during a month is small enough to have no significant effect on the monthly means and thus they indeed characterize the background conditions. This assumption is also supported by the fact that the PATMOS products were generated from GAC data, which are the result of a spatial sampling and averaging of 1-km measurements and thus are less influenced by the signal from small hot spots.

[15] The current continuous record of 1-km AVHRR data at NOAA (<http://www.saa.noaa.gov>) goes back to May 1985, while 1-km data from the earlier years are scarce. From the ~ 20 years covered by the PATMOS data set, our primary concern here is the 1985–2000 period (i.e., NOAA 9, 11 and 14).

[16] A potential alternative data set for the long-term time series analysis is the AVHRR Pathfinder Land I data set [James and Kalluri, 1994], which also includes channel 3 measurements at 8-km resolution. However, for the objective of this paper the lower resolution information on background conditions from PATMOS was sufficient; in fact, this study would have needed the temporal and spatial aggregation of the 8-km data to a product similar to the PATMOS monthly means.

3. Interannual Changes of Background Brightness Temperatures

[17] A primary requirement for successful active fire detection is the distinct separation of the fire signal from the background. Even small fires substantially elevate and often saturate the midinfrared channel, whereas the infrared window channel is far less sensitive to the presence of subpixel hot spots. As a consequence, T3–T4 differencing is an important element of most AVHRR-based active fire detection techniques. In the remainder of the text, T3–T4 will be listed as ΔT_{34} .

[18] Note that, if the size of the hot spot is comparable to the pixel size of the satellite sensor, T4 also increases substantially [Dozier, 1981; Kaufman *et al.*, 1998; Giglio *et al.*, 1999; Li *et al.*, 2001]. Although even in this situation the temperature difference does not vanish completely because of the remaining additional reflected solar component in the midinfrared, the ΔT_{34} test is no longer applicable. However, this rarely occurs for moderate resolution sensors like AVHRR.

[19] If the background temperature increases, ΔT_{34} becomes smaller if and when T3 reaches the saturation temperature of ~ 322 K (T4 almost never reaches this value). In this situation the fire detection algorithms will tend to reject valid fire pixels along with hot/bright surfaces, resulting in omission errors. If, however, the ΔT_{34} threshold is decreased accordingly to accommodate valid fires, the likelihood of detecting false fires (commission errors) will increase. Ideally, for successful active fire detection using AVHRR, the background T3 should not reach the saturation temperature.

[20] Note that the use of contextual heterogeneity tests [e.g., Flasse and Ceccato, 1996; Justice *et al.*, 1996], which derive dynamic thresholds from the background temperature conditions, may decrease but can not fully resolve the above ambiguity because (1) they are still based on

the assumption of a statistically significant contrast between the potential fire pixel and its surroundings and (2) with the increasing background temperature the separation of adjacent fire pixels and a fire-free background pixel becomes ambiguous. While they indeed tend to eliminate false alarms from uniformly hot areas, commission errors can remain at the edges of hot surfaces or clouds [Giglio *et al.*, 1999; Li *et al.*, 2000b].

[21] Figures 2a–2d show time series of AVHRR channel 3 and channel 4 monthly mean temperatures in July over different target areas in the western United States, with the corresponding ± 1 standard deviations from PATMOS. July cases are shown to represent the extreme high temperature conditions and also the peak of the North American fire season. Note that the higher monthly mean T3 values compared to the coincident channel 4 temperatures are caused not by fire hot spots but rather by the solar reflection component in the midinfrared radiance, which is known to be a major cause of commission errors in daytime fire detection.

[22] The target areas were chosen to characterize different vegetation classes. The predominant land cover types were determined from the International Geosphere-Biosphere Programme (IGBP) global 1 km land cover data set [Love-land *et al.*, 2000]. In this data set, forest cover is defined as percent tree canopy cover $>60\%$, and height exceeding 2 m [Hansen *et al.*, 2000].

[23] All the plots show some degree of interannual variability; however, the effect of this on the detection accuracy is different. Over the grid cell that covers forested areas in Montana (mean elevation ~ 1600 m), although considerable differences exist (up to 15 K), in all years the background temperatures are low enough to allow an unambiguous separation of fire signals from the background. Over croplands in Kansas (Figure 2b; elevation ~ 360 m) there is again a substantial interannual fluctuation. T3 still never reaches the saturation temperature, but in some years, particularly in 1991, it gets high enough to anticipate difficulties in separating hot spots from the background. Over open shrublands in NW Utah (Figure 2c; elevation ~ 1400 m), T3 basically hits the upper threshold in about half of the years, leading to a decrease in both T3–T4 and detection certainty. The sparsely vegetated Arizona target (Figure 2d; elevation ~ 500 m) shows saturated T3 values for almost all of the years, with T3–T4 decreasing to only 1–2 K in 1995 and 1997. Fire detection in such areas is extremely difficult using the thermal channels of AVHRR.

[24] The above data are plotted in a different perspective in Figure 3. Filled circles denote the quantity $[322(\text{K}) - T_4]$, which can be seen as an estimate of the upper limit of the physically possible ΔT_{34} for a 1-km pixel representing fire hot spots in that particular year and month and within that particular $1^\circ \times 1^\circ$ area. This quantity is compared with the background ΔT_{34} (triangles). Note that standard deviations are not shown, because they could not be readily derived from the monthly PATMOS data set. The separability of fires from background can be illustrated by the difference between these two quantities. In principle, the ΔT_{34} threshold in a fire detection algorithm should be placed between them, optimally closer to the background ΔT_{34} value to accommodate smaller fires that

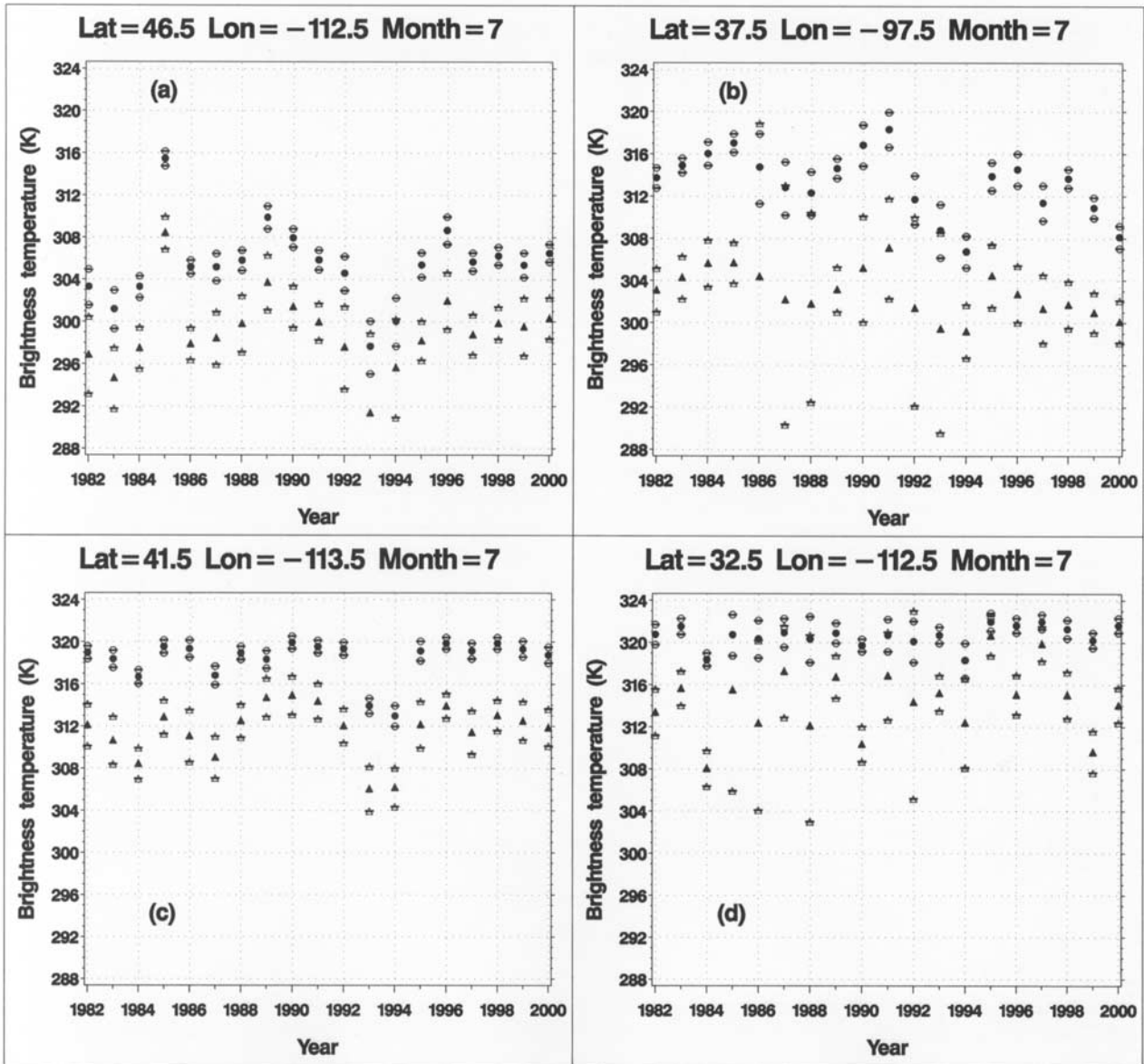


Figure 2. Time series of AVHRR channel 3 and channel 4 monthly mean brightness temperatures (filled circles and triangles respectively) and ± 1 standard deviations (open symbols superimposed by dash) in July over a $1^\circ \times 1^\circ$ grid cells in (a) Montana, (b) Kansas, (c) NW Utah and (d) Arizona.

do not saturate channel 3. The Montana target shows clear separation, except for 1985, when the algorithms with more conservative thresholds may fail. There is still a relatively large gap for the Kansas target area. However, it is obvious that a constant threshold (optimally at $\sim 13\text{--}14$ K) over the years occasionally may result in ambiguities. Both the NW Utah and Arizona targets exhibit little or no difference and high interannual variability, pointing out the difficulties in establishing an appropriate ΔT_{34} threshold there.

[25] From the point of view of deriving a long-term record of active fires in North America, the above analysis demonstrates the feasibility of producing a consistent, accurate time series of fires over forested areas, while arid regions should be excluded from the analysis. In addition,

fires are rare in deserts and other highly arid regions due to the absence or very low amount of fuel from vegetation. The more significant problem areas are the transitional land cover types, such as grassland, pasture, or cropland, where there is still fuel available for large fires. As shown above, while detection accuracy in some years is expected to be similar to that in forested areas, in other years the background temperature conditions are such that they severely limit the potential for accurate fire detection.

[26] In midlatitudes, we generally note that it is the amount of fuel (i.e., vegetation) itself that determines the potential for successful fire detection. Besides this primary factor, a secondary effect is the vegetation condition. In drought conditions, with higher fire risk and occurrence, background temperature and reflectivity increase over the

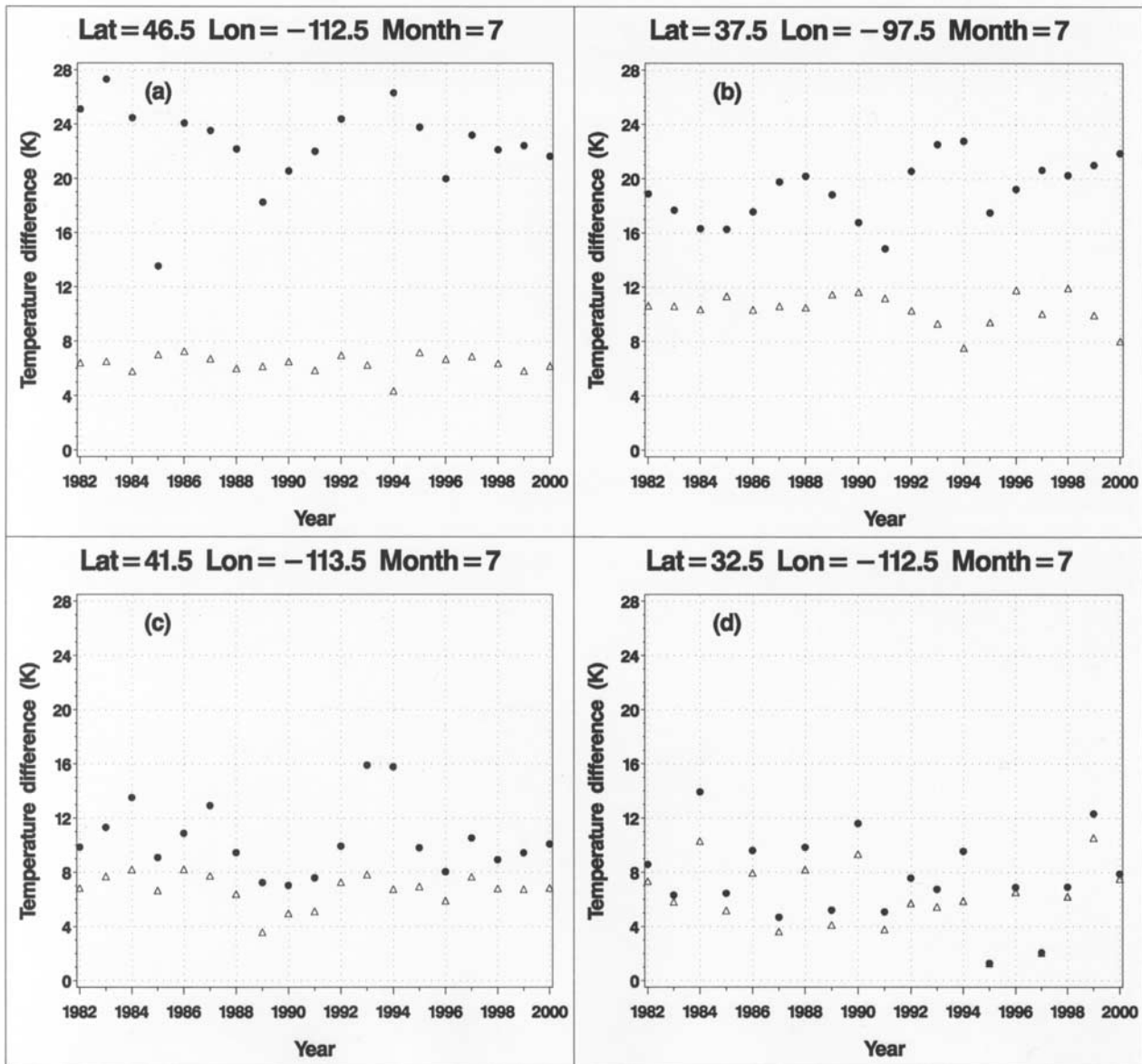


Figure 3. Time series of AVHRR temperatures in July over a $1^\circ \times 1^\circ$ grid cells in (a) Montana, (b) Kansas, (c) NW Utah and (d) Arizona. Filled circles: [322-T4]; triangles: ΔT_{34} .

same area as compared to normal conditions, decreasing the detection accuracy. An example is shown in Figure 4 over grassland in Oklahoma (elevation ~ 200 m) in July. The years with abnormally high background brightness temperatures coincide with those identified as having stressed vegetation condition by the NOAA/NESDIS Vegetation Health by Climate Division product (<http://orbit-net.nesdis.noaa.gov/crad/sat/surf/vci/iscd/usacd.html>), particularly in 1998. In that year the background T3 value was ~ 3 degrees above normal and almost reached the saturation temperature.

[27] All the above results and conclusions need to be considered in the light of the fact that active fire detection is best applied as confirmation or validation tool towards burned area estimates. Burned area mapping techniques identify areas as burned only where significant surface changes occur. In principle, our active fire mapping efforts

need to be directed towards minimizing omission errors, expecting many false fire signals, particularly from hot surfaces, to be discarded by the burned area mapping algorithms.

4. Burning Over Nonforested Areas

[28] The results presented in section 3 indicate that while active fire detection over forests appears to be sufficiently robust to ensure minimum omission and commission errors that are consistent over multiple years, nonforested areas represent difficulties both in instantaneous active fire detection and in deriving a long-term, homogeneous time series. This raises the question whether efforts should be taken to process nonforested areas considering the risk of introducing false signals in the time series. To answer this question, a detailed analysis of the contribution of nonforest

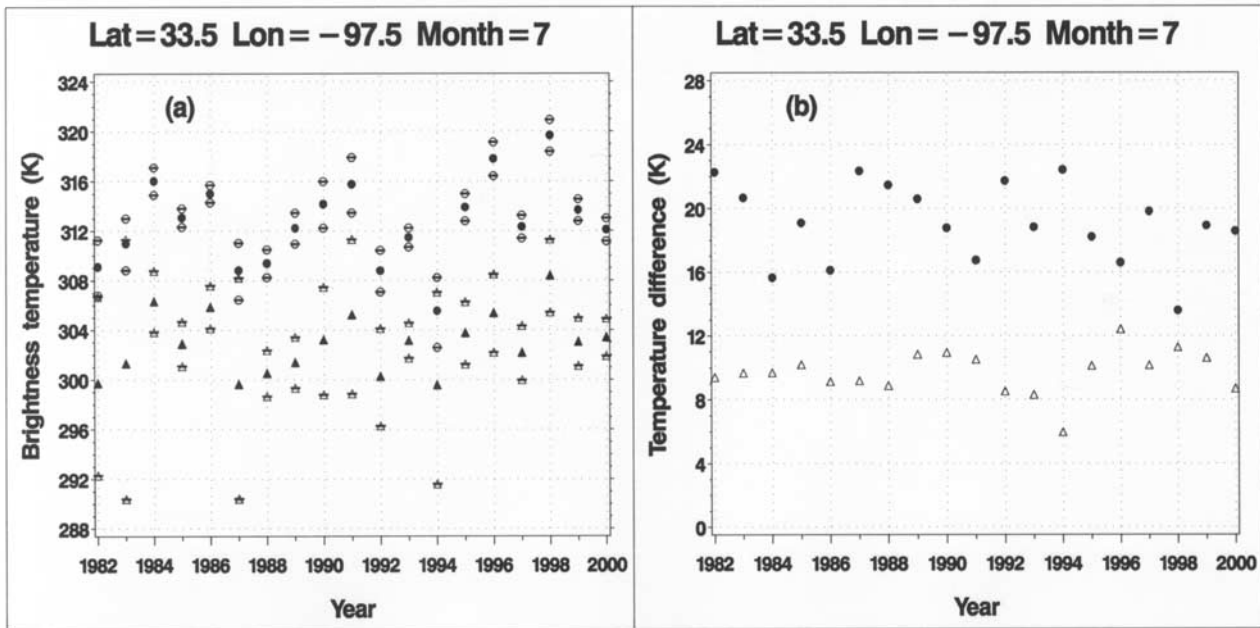


Figure 4. (a) Time series of AVHRR channel 3 and channel 4 monthly mean brightness temperatures (filled circles and triangles respectively) and ± 1 standard deviations (open symbols superimposed by dash) in July over a $1^\circ \times 1^\circ$ grid cell in Oklahoma. Higher than normal temperatures in 1996 and 1998 indicate drought conditions. (b) Corresponding [322-T4] (filled circles) and ΔT_{34} (triangles).

fires to the total fire emissions needs to be performed along with the assessment of fire impacts on land cover change in these regions. This task is beyond the scope of this paper. Here we present only an illustration of the problem using the case of NW U.S. fires during 2000, when both widespread forest fires and rapidly advancing brush fires occurred [Ramsey and Arrowsmith, 2001]. Figure 5 shows the cumulative daily detection of fires throughout the 2000 fire season in the area. The reference burned area polygons were derived by ground and airborne GPS surveys carried out by the U.S. Forest Service (<http://www.fs.fed.us/r1/ecology/fire2000>).

[29] In the database each polygon is flagged with the first day of burning. Red points on the map indicate fire detection locations from AVHRR by the CCRS (Canada Center for Remote Sensing) algorithm. This technique was originally developed and used for fire mapping over the Canadian boreal forests [Li *et al.*, 2000a, 2000b] and later modified for continental-scale monitoring over North America [Li *et al.*, 2002]. Shades of green denote various types of forest cover. Most of the nonforested area in the scene is open shrubland or cropland. It can be seen that in the forested areas of Idaho and Montana, where most of the burning in 2000 took place, fires were quite accurately detected using the satellite [Li *et al.*, 2002]. Over other surfaces, however, CCRS fire detection produced many apparent false alarms, together with some real fire signal within the USFS polygons. Overall there is little correspondence between the fire locations and the USFS polygons over nonforested areas.

[30] Now we focus on two large USFS polygons within the open shrubland area. Figure 6 shows red-green-blue (RGB) color composites of the zoomed area created from

AVHRR level-1b data. The starting dates of the fires within the lower right and upper left areas are July 1 and 17, respectively. For the second fire, images from July 18 are shown here, because the July 17 NOAA 14 image was cloudy. The top images show channel 3-2-1 RGB composites, where hot areas are depicted as red, green color indicates vegetation, and smoke from fires is blue. One can see that the burned polygons have high T3 values, both because of actual burning and smoldering, and because of the higher absorption and thus heating from the charred burned surface.

[31] The 1-2-4 RGB images on the bottom show the darkening of the burned areas, particularly in the green (near-IR), which is the physical basis of burned area detection. On both color composites distinct smoke plumes are visible, indicating substantial particulate emission. It is also remarkable that within a short period a relatively large area burned, suggesting a fast movement of the fire front and consequently substantial total fuel consumption, despite the fact that the fuel loading per unit area is obviously lower than in forests. The above examples intuitively indicate that the exclusion of burning over nonforested areas may result in a nonnegligible underestimation of emissions from fires.

5. Conclusions

[32] The above analysis has demonstrated that, for the purpose of long-term studies, the compromise between omission and commission errors is aggravated by the need of ensuring that the errors remain consistent over time. Nonforested areas are most affected by the instability attributable to interannual changes in Sun-satellite-sensor

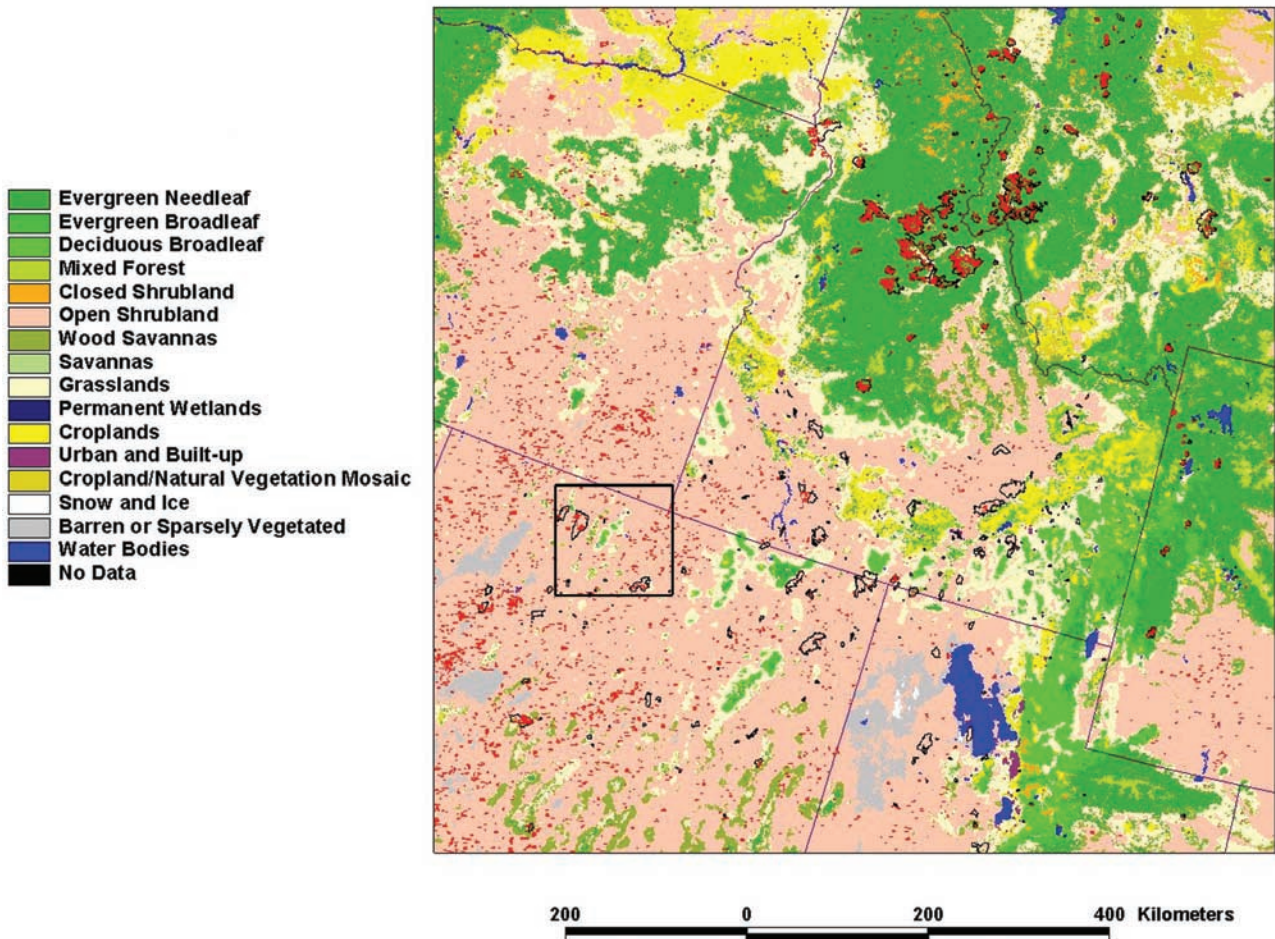


Figure 5. Yearly cumulative burned areas in NW United States. The polygons are results of the U.S. Forest Service survey. Red color indicates fire detection by the latest CCRS algorithm. The land cover classes are from the IGBP-DIS 1 km global land cover data set. The outlined area is shown in Figure 6.

configuration. Thus they represent a major uncertainty in terms of long-term, large-scale emission estimates from fires. This uncertainty can be minimized through a rigorous analysis of spatial and temporal changes affecting fire detection accuracy and the development of variable temperature and reflectance thresholds [Cuomo *et al.*, 2001]. In fact, a comprehensive analysis similar to that presented in Section 3 can help establish absolute temperature thresholds for the identification of potential fire pixels (Figure 2), thresholds for ΔT_{34} to separate fires from false alarms (Figure 3) and even a measure of confidence based on the ambiguity of the signal. There is also the potential of combining hotspot detection with identification of smoke aerosol in the neighboring pixels. For such an analysis the development of a high-resolution database of visible reflectances is needed for a number of Sun-target-sensor geometries to account for bidirectional effects [Knapp and Stowe, 2002].

[33] In addition to the effects discussed in this paper, other factors may also cause interannual variability of error characteristics of the fire products. Research is also under way to understand the importance of the year-to-year change of the occurrence of sun-glint conditions. Changes

in post-launch calibration caused by sensor degradation may also need to be accounted for. In areas of heavy agricultural burning, such as the Mississippi Valley and the southeast United States, as well as tropical areas of marked diurnal fire cycle, the orbital drift-related changes in diurnal sampling need to be addressed also.

[34] This study has focused on North America, where nearly complete coverage of 1-km AVHRR data is available since 1985. This analysis can be extended to other areas of the world towards the assessment of the potential of a retrospective, global AVHRR-based fire mapping. In the global context, surface types not present in North America, such as tree and shrub savannas with the highest fire activity, need to be thoroughly analyzed.

[35] An ideal approach to eliminate the potential sources of detection error discussed in this paper would be to use nighttime observations for fire detection. Paradoxically, however, fires over nonforested areas, which exhibit most of the detection errors, tend to occur during daytime and are of shorter duration. Many of them would therefore be missed by this approach.

[36] With the advent of the new generation of mid-IR sensors with higher saturation temperatures, including

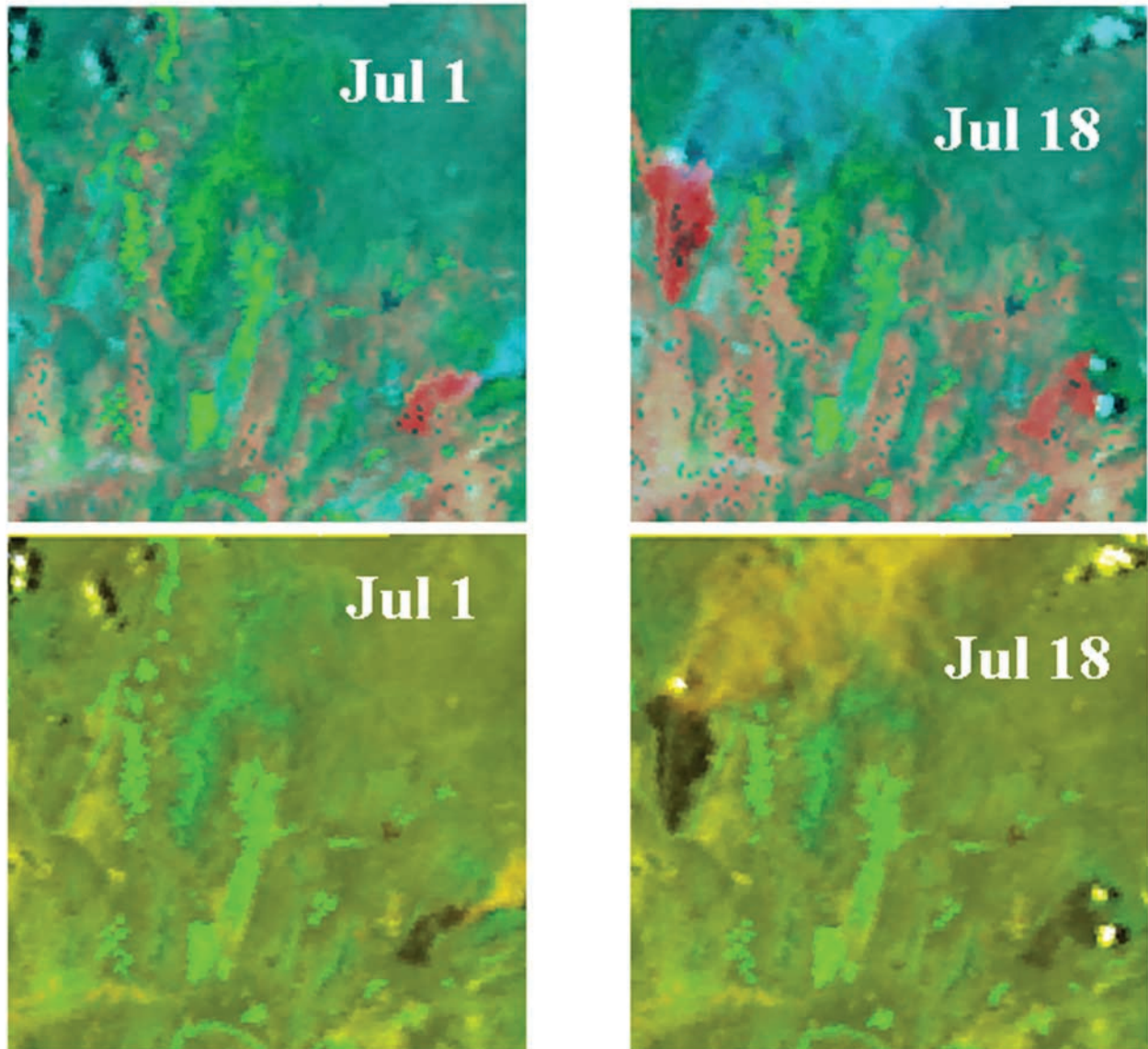


Figure 6. (top) Color composite images (mid-IR, near-IR, visible = R, G, B) on days of intense biomass burning in NW Utah. (bottom) red (visible) - green (near-IR) - blue (IR) images of the areas on the same dates. The area is outlined in Figure 5. See text for details.

AVHRR/3 on board the NOAA satellites (NOAA 15 and later) and particularly MODIS on board the NASA Earth Observing System Terra and Aqua satellites, most of the issues discussed in this paper have been eliminated. However, NOAA/AVHRR is the only sensor that can be used for large-scale fire mapping over the 1985–2000 period. Efforts should also be directed at understanding the relationship between the active fire and burned area products from AVHRR/2 and the new sensors [Justice and Korontzi, 2001].

[37] **Acknowledgments.** We thank the PATMOS team led by L Stowe (NOAA/NESDIS/ORA) for making the data set available and for valuable comments on its use. Thanks go to W. Emery and D. Baldwin (University of Colorado at Boulder) for providing their navigation software for remapping AVHRR data. This work was supported by the NASA Land Cover Land Use Change grant NRA-99-OES-06 “Development of a Long

Term Inventory of Fire Burned Areas and Emissions of North America’s Boreal and Temperate Forests.”

References

- Andreae, M. O., and P. Merlet, Emissions of trace gases and aerosols from biomass burning, *Global Biogeochem. Cycles*, 15, 955–966, 2001.
- Arino, O., M. Simon, I. Piccolini, and J. M. Rosaz, The ERS-2 ATSR-2 World Fire Atlas and the ERS-2 ATSR-2 World Burnt Surface Atlas projects, paper presented at 8th ISPRS Conference on Physical Measurement and Signatures in Remote Sensing, Int. Soc. for Photogramm. and Remote Sens., Aussois, 8–12 Jan. 2001.
- Barbosa, P. M., J.-M. Grégoire, and J. M. C. Pereira, An algorithm for extracting burned areas from time series of AVHRR GAC data applied at a continental scale, *Remote Sens. Environ.*, 69, 253–263, 1999.
- Belward, A. S., P. J. Kennedy, and J. M. Grégoire, The limitations and potential of AVHRR GAC for continental scale fire studies, *Int. J. Remote Sens.*, 15, 2215–2234, 1994.
- Cihlar, J., Land cover mapping of large areas from satellites: Status and research priorities, *Int. J. Remote Sens.*, 21, 1093–1114, 2000.

- Cofer, W. R., E. L. Winstead, B. J. Stocks, L. W. Overbay, J. G. Goldammer, D. R. Cahoon, and J. S. Levine, Emissions from boreal forest fires: Are the atmospheric impacts underestimated?, in *Biomass Burning*, edited by J. S. Levine, pp. 834–839, MIT Press, Cambridge, Mass., 1996.
- Csiszar, I., and J. Sullivan, Recalculated pre-launch saturation temperatures of the AVHRR 3.7 μm sensors on board the TIROS-N to NOAA-14 satellites, *Int. J. Remote Sens.*, in press, 2002.
- Cuomo, V., R. Lasaponara, and V. Tramutoli, Evaluation of a new satellite-based method for forest fire detection, *Int. J. Remote Sens.*, 22, 1799–1826, 2001.
- Dozier, J., A method for satellite identification of surface temperature fields of subpixel resolution, *Remote Sens. Environ.*, 11, 221–229, 1981.
- Dwyer, E., S. Pinnock, and J.-M. Grégoire, Global spatial and temporal distribution of vegetation fire as determined from satellite observations, *Int. J. Remote Sens.*, 21, 1289–1302, 2000.
- El Saleous, N. Z., E. F. Vermote, C. O. Justice, J. R. G. Townshend, C. J. Tucker, and S. N. Goward, Improvements in the global biospheric record from the advanced very high resolution radiometer (AVHRR), *Int. J. Remote Sens.*, 21, 1251–1277, 2000.
- Elvidge, C. D., I. Nelson, V. R. Hobson, J. Safran, and K. E. Baugh, Detection of fires at night using DMSP-OLS data, in *Global and Regional Fire Monitoring From Space: Planning a Coordinated International Effort*, edited by F. Ahern, J. Goldammer, and C. O. Justice, pp. 125–144, SPB Academic, The Hague, 2001.
- Fearnside, P. M., Global warming and tropical land-use change: Greenhouse gas emissions from biomass burning, decomposition and soils in forest conversion, shifting cultivation and secondary vegetation, *Clim. Change*, 46, 115–158, 2000.
- Fernandez, A., P. Illera, and J. L. Casanova, Automatic mapping of surfaces affected by forest fires in Spain using AVHRR NDVI composite image data, *Remote Sens. Environ.*, 60, 153–162, 1997.
- Flasse, S. P., and P. Ceccato, A contextual algorithm for AVHRR fire detection, *Int. J. Remote Sens.*, 17, 419–424, 1996.
- Franca, H., and A. W. Setzer, AVHRR analysis of a savanna site through a fire season in Brazil, *Int. J. Remote Sens.*, 22, 2449–2461, 2001.
- Fraser, R. H., Z. Li, and J. Cihlar, Hotspot and NDVI Differencing (HANDS): A new technique for burned area mapping over boreal forest, *Remote Sens. Environ.*, 74, 362–376, 2000.
- Giglio, L., J. D. Kendall, and C. O. Justice, Evaluation of global fire detection using simulated AVHRR infrared data, *Int. J. Remote Sens.*, 20, 1947–1985, 1999.
- Grégoire, J.-M., A. S. Belward, and P. Kennedy, Dynamiques de saturation du signal dans la bande 3 du senseur AVHRR: Handicap majeur ou source d'information pour la surveillance de l'environnement en milieu soudanoguinéen d'Afrique de l'Ouest?, *Int. J. Remote Sens.*, 14, 2079–2095, 1993.
- Grégoire, J.-M., D. R. Cahoon, D. Stroppiana, Z. Li, S. Pinnock, H. Eva, O. Arino, J.-M. Rosza, and I. Csiszar, Forest fire monitoring and mapping for GOF: Current products and information networks based on NOAA-AVHRR, ERS-ATSR, and SPOT-VGT systems, in *Global and Regional Fire Monitoring From Space: Planning a Coordinated International Effort*, edited by F. Ahern, J. Goldammer, and C. O. Justice, pp. 105–124, SPB Academic, The Hague, 2001.
- Gutman, G., I. Csiszar, and P. Romanov, Using NOAA/AVHRR products to monitor El Niño impacts: Focus on Indonesia in 1997–1998, *Bull. Am. Meteorol. Soc.*, 81, 1189–1205, 2000.
- Gutman, G., C. Elvidge, I. Csiszar, and P. Romanov, NOAA archives of data from meteorological satellites useful for fire products, in *Global and Regional Fire Monitoring From Space: Planning a Coordinated International Effort*, edited by F. Ahern, J. Goldammer, and C. O. Justice, pp. 257–266, SPB Academic, The Hague, 2001.
- Hansen, M. C., R. S. DeFries, J. R. G. Townshend, and R. Sohlberg, Global land cover classification at 1 km spatial resolution using a classification tree approach, *Int. J. Remote Sens.*, 21, 1331–1364, 2000.
- Hao, W.-M., D. W. Ward, G. Olbu, and S. P. Baker, Emissions of CO₂, CO, and hydrocarbons from fires in diverse African savanna ecosystems, *J. Geophys. Res.*, 101, 23,577–23,584, 1996.
- Harris, A. J. L., D. A. Rothery, R. W. Carlton, S. Langaas, and H. Manstein, Non-zero saturation of AVHRR thermal channels over high temperature targets: Evidence from volcano data and a possible explanation, *Int. J. Remote Sens.*, 16, 189–196, 1995.
- James, M. E., and S. N. V. Kalluri, The Pathfinder AVHRR land data set: An improved coarse resolution data set for terrestrial monitoring, *Int. J. Remote Sens.*, 15, 3347–3363, 1994.
- Justice, C. O., and S. Korontzi, A review of the status of satellite fire monitoring and the requirements for global environmental change research, in *Global and Regional Fire Monitoring From Space: Planning a Coordinated International Effort*, edited by F. Ahern, J. Goldammer, and C. O. Justice, pp. 1–18, SPB Academic, The Hague, 2001.
- Justice, C. O., J. D. Kendall, P. R. Dowty, and R. J. Scholes, Satellite remote sensing of fires during the SAFARI campaign using NOAA advanced very high resolution radiometer data, *J. Geophys. Res.*, 101, 23,851–23,863, 1996.
- Kaufman, Y. J., C. Justice, L. Flynn, J. Kendall, E. Prins, D. E. Ward, P. Menzel, and A. Setzer, Potential global fire monitoring from EOS-MODIS, *J. Geophys. Res.*, 103, 32,215–32,238, 1998.
- Kidwell, K. B., (Ed.), NOAA Polar Orbiter data users guide, <http://lwf.ncdc.noaa.gov/oa/ncdc.html>, Natl. Clim. Data Cent., Asheville, North Carolina, 1998.
- Knapp, K. R., and L. L. Stowe, Evaluating the potential for retrieving aerosol optical depth over land from AVHRR Pathfinder Atmosphere data, *J. Atmos. Sci.*, 59, 279–293, 2002.
- Li, Z., S. Nadon, and J. Cihlar, Satellite detection of Canadian boreal forest fires: Development and application of an algorithm, *Int. J. Remote Sens.*, 21, 3057–3069, 2000a.
- Li, Z., S. Nadon, J. Cihlar, and B. J. Stocks, Satellite mapping of Canadian boreal forest fires: Evaluation and comparison of algorithms, *Int. J. Remote Sens.*, 21, 3071–3082, 2000b.
- Li, Z., Y. J. Kaufman, C. Ichoku, R. Fraser, A. Trishchenko, L. Giglio, J.-Z. Jin, and X. Yu, A review of satellite fire detection algorithms: principles, limitations and recommendations, in *Global and Regional Fire Monitoring From Space: Planning a Coordinated International Effort*, edited by F. Ahern, J. Goldammer, and C. O. Justice, pp. 199–226, SPB Academic, The Hague, 2001.
- Li, Z., R. Fraser, J. Jin, A. Abuelgasim, I. Csiszar, P. Gong, and W.-M. Hao, Evaluation of satellite-based algorithms for fire detection and mapping within North America, *J. Geophys. Res.*, doi:10.1029/2001JD001377, in press, 2002.
- Lobert, J. M., W. C. Keene, J. A. Logan, and R. Yevich, Global chlorine emissions from biomass burning: Reactive Chlorine Emissions Inventory, *J. Geophys. Res.*, 104, 8373–8389, 1999.
- Loveland, T. R., B. C. Reed, J. F. Brown, D. O. Ohlen, Z. Zhu, L. Yang, and J. W. Merchant, Development of a global land cover characteristics database and IGBP DISCover from 1 km AVHRR data, *Int. J. Remote Sens.*, 21, 1303–1330, 2000.
- Prins, E. M., J. M. Feltz, W. P. Menzel, and D. E. Ward, An overview of GOES-8 diurnal fire and smoke results for SCAR-B and the 1995 fire season in South America, *J. Geophys. Res.*, 103, 31,821–31,836, 1998.
- Ramsey, M. S., and J. R. Arrowsmith, New images of fire scars may help mitigate future natural hazards, *Eos Trans. AGU*, 82(36), 393, 397–398, 2001.
- Robinson, J. M., Fire from space: Global evaluation using infrared remote sensing, *Int. J. Remote Sens.*, 12, 3–24, 1991.
- Roy, D. P., and P. E. Lewis, Burned area mapping from multitemporal surface bidirectional reflectance, *Eos Trans. AGU*, 81(19), S393, Spring Meet. Suppl., 2000.
- Setzer, A. W., and M. M. Verstraete, Fire and glint in AVHRR's channel 3: A possible reason for the non-saturation mystery, *Int. J. Remote Sens.*, 15, 711–718, 1994.
- Stowe, L. L., H. Jacobowitz, G. Ohring, K. R. Knapp, and N. R. Nalli, The advanced very high resolution radiometer Pathfinder Atmosphere (PATMOS) data set: Initial analyses and evaluations, *J. Clim.*, 15, 1243–1260, 2002.
- Stroppiana, D., S. Pinnock, and J.-M. Grégoire, The Global Fire Product: Daily fire occurrence from April 1992 to December 1993 derived from NOAA AVHRR data, *Int. J. Remote Sens.*, 21, 1279–1288, 2000.
- Zhan, X., R. Defries, J. R. G. Townshend, C. Dimiceli, M. Hansen, C. Huang, and R. Sohlberg, The 250 m global land cover change product from the Moderate Resolution Imaging Spectroradiometer of NASA's Earth Observing System, *Int. J. Remote Sens.*, 21, 1433–1460, 2000.

A. Abuelgasim, Noetix Research Inc., Environmental Monitoring Section, AD, Canada Center for Remote Sensing, 588 Booth Street, Ottawa, Ontario K1A 0Y7, Canada.

I. Csiszar, Department of Geography, University of Maryland, 1121 LeFrak Hall, College Park, MD 20742, USA. (iciszar@hermes.geog.umd.edu)

R. Fraser, Environmental Monitoring Section, Canada Center for Remote Sensing, 588 Booth Street, Ottawa, Ontario K1A 0Y7, Canada.
W.-M. Hao, Fire Sciences Laboratory, Rocky Mountain Research Station, USDA Forest Service, P. O. Box 8089, Missoula, MT 59807, USA. (whao/rmrs_missoula@fs.fed.us)

J. Jin and Z. Li, Department of Meteorology, Earth System Science Interdisciplinary Center, University of Maryland, 2335 Computer and Science Building, College Park, MD 20742, USA. (jzhongjin@yahoo.com; zli@atmos.umd.edu)